Catal Lett (2008) 123:213–219
DOI 10.1007/s10562-008-9453-1

Synthesis of Ionones by Cyclization of Pseudoionone on Solid Acid Catalysts

V. K. Díez · C. R. Apesteguía · J. I. Di Cosimo

Received: 8 February 2008 / Accepted: 27 February 2008 / Published online: 14 March 2008

Abstract Ionone synthesis (α, β and γ isomers) by pseudoionone cyclization was studied on zeolite HBEA, Amberlyst 35W, SiO_2–Al_2O_3, and unsupported and silica-supported heteropolyacids (HPA/SiO_2). Ionone formation was preferentially promoted on strong Brønsted acid sites. A 79% ionone yield was obtained on 58.5 wt.% HPA/SiO_2 after 1.5 h of reaction at 383 K and 250 kPa. This value is similar to the best yields reported for the homogeneously-catalyzed reaction using sulfuric acid.

Keywords Ionone · Heteropolyacid · Acid catalysis · Tungstophosphoric acid

1 Introduction

Among citral-derived compounds, ionones are extensively used as pharmaceuticals and fragrances. The β-ionone isomer is the preferred reactant for different synthesis processes leading to vitamin A, whereas α- and γ-ionones are very appreciated in the fragrance industry because of their violet and woody-fruity scent, respectively [1, 2].

Ionones are commercially produced from citral via a two-step homogeneous process, as depicted in Scheme 1. In the first step, the aldol condensation of citral with acetone to give pseudoionone (PS) is catalyzed by diluted bases such as NaOH, $Ba(OH)_2$, and LiOH. The consecutive liquid-phase cyclization of PS to ionones is catalyzed by mineral acids [3]. Because of the use of harmful liquid catalysts, the ionone synthesis shown in Scheme 1 entails concerns related to high toxicity, corrosion, and disposal of spent base and acid materials.

Ionone yields of 70–90% have been reported for the PS cyclization using liquid acids [3–7]. The acid catalyst nature (Lewis or Brønsted), concentration and strength determine the ionone isomer distribution [4]. For instance, concentrated sulfuric acid produces predominantly β-ionone [5–7] while phosphoric acid forms essentially α-ionone [3]. In contrast, γ-ionone is the main isomer when Lewis acids such as BF_3 are used [8].

In spite of the interest for developing ecofriendly heterogeneous processes to obtain ionones by PS cyclization, there are very few papers in literature on the use of solid acids for this reaction. In fact, it has been reported only recently that strongly acidic resins [9] and sulfated and persulfated TiO_2/MCM-41 [10] promote the PS conversion to ionones. However, the ionone yields (30–49%) were significantly lower than those obtained via the homogeneous reaction.

In this paper we studied the liquid-phase cyclization of PS to ionones on bulk HPA, HPA/SiO_2, Cs-HPA, zeolite

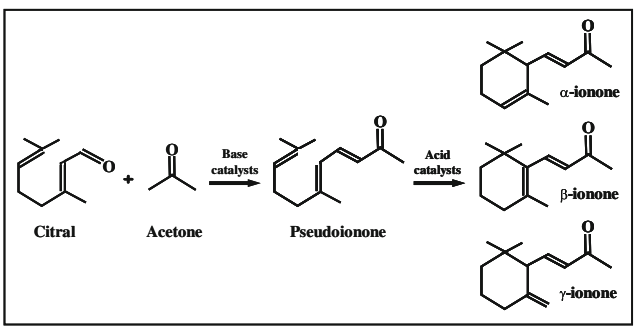

Scheme 1 Two-step process for ionone synthesis

V. K. Díez · C. R. Apesteguía · J. I. Di Cosimo (✉)
Catalysis Science and Engineering Research Group (GICIC), INCAPE, UNL-CONICET, Santiago del Estero 2654, 3000 Santa Fe, Argentina
e-mail: dicosimo@fiq.unl.edu.ar

HBEA, SiO_2–Al_2O_3 and Amberlyst 35W. The catalyst acid properties were determined by FTIR of pyridine. Results show that the reaction was efficiently promoted on strong Brønsted acid sites with HPA/SiO_2 being the most active and selective catalyst. In-situ catalyst deactivation studies showed a slight deactivation of the HPA/SiO_2 catalysts during reaction that cannot be attributed to HPA leaching. A proper selection of the HPA loading, reaction time, conversion level, reaction temperature and solvent is crucial in order to improve the catalyst activity and to control the ionone isomer distribution (α, β and γ). Ionone yields of up to 79% were obtained. To the best of our knowledge, this is the first time a value comparable to those of the homogeneous process using sulfuric acid is reported using a solid acid catalyst.

2 Experimental

HPA/SiO_2 catalysts were prepared by incipient wetness impregnation method. The tungstophosphoric acid ($H_3PW_{12}O_{40} \cdot xH_2O$, Merck, GR) was added to a commercial SiO_2 (Grace Davison, G62, 99.7%, 272 m^2/g, pore diameter = 122 Å) using an aqueous solution of HPA. Then samples were dried at 353 K and finally decomposed and stabilized at 523 K for 18 h in flowing N_2. The cesium salt of the tungstophosphoric acid ($Cs_{2.5}H_{0.5}PW_{12}O_{40}$, Cs-HPA sample) was prepared by slowly adding an aqueous solution of Cs_2CO_3 (Sigma-Aldrich, PA 99.9%) to an aqueous solution of $H_3PW_{12}O_{40}$. The precipitate was heated overnight at 353 K and then calcined in N_2 flow at 573 K. Structural properties of the HPA-derived solids were analyzed by X-ray diffraction (XRD) using a Shimadzu XD-D1 equipped with Cu-Kα radiation and a Ni filter.

$SiO_2-Al_2O_3$ (powder, Sigma-Aldrich, Si/Al = 6.6 molar ratio) and zeolite HBEA (powder, Zeocat PB/H, Si/Al = 12.5 molar ratio) were treated in air at 723 K before the catalytic and spectroscopic experiments. Amberlyst 35W (700–950 μ beads, Rohm and Haas) were treated in N_2 flow at 373 K.

Elemental compositions were measured using atomic absorption spectroscopy. The HPA content in HPA/SiO_2 catalysts was determined by UV spectroscopy [11] with a Metrolab 1700 UV–vis spectrometer. BET surface areas were measured by N_2 physisorption at its boiling point using an Autosorb Quantachrome 1-C sorptometer.

The chemical nature of surface acid sites was determined by Infrared Spectroscopy (IR) by using pyridine as probe molecule and a Shimadzu FTIR Prestige-21 spectrophotometer. Sample wafers were evacuated at the calcination temperature, then cooled down to room temperature to take the catalyst spectrum. After exposure to 0.12 kPa of pyridine at room temperature samples were evacuated consecutively at 298, 423, 573, and 723 K (zeolite HBEA and SiO_2–Al_2O_3) or at 298, 373, 423 and 473 K (HPA-based samples) and the resulting spectrum was recorded at room temperature. Spectra of the adsorbed species were obtained by subtracting the catalyst spectrum.

The cyclization of pseudoionone (Fluka, >90%) was carried out at 353–383 K under autogenous pressure ($\approx$250 kPa) in a batch PARR reactor, using aprotic solvents and a catalyst/PS = 56 wt.% ratio. The batch reactor was assumed to be perfectly mixed. Catalysts were loaded as ground powders (except Amberlyst 35W) in which inter- and intra-particle diffusional limitations were verified to be negligible.

Reaction products were periodically analyzed during the 6-h reaction in a Varian Star 3400 CX gas chromatograph equipped with an FID and a Carbowax Amine 30 M capillary column. Main reaction products were ionones (α, β and γ isomers). Product selectivities (S_j, mol of product j/mol of PS reacted) were calculated as $S_j = C_j/\Sigma C_j$ where C_j is the concentration of product j. Product yields (η_j, mol of product j/mol of PS fed) were calculated as $\eta_j = S_j \times X_{PS}$, where X_{PS} is the pseudoionone conversion. Initial ionone formation rate (r^0_{IONONE}) was calculated from the initial slope of the η_{IONONE} vs. time curve.

3 Results and Discussion

3.1 Catalyst Characterization and Selection

The chemical composition, BET surface area and acid properties of the catalysts are presented in Table 1. Bulk commercial HPA had a low surface area (9 m^2/g), but replacement of most of the heteropolyacid protons by Cs^+ in the HPA structure increased the surface area to 143 m^2/g (Cs-HPA sample), which is in agreement with previous reports [12]. Regarding the 42.5 wt.% HPA/SiO_2 sample, addition of bulky HPA molecules caused a significant diminution of the SiO_2 surface area, from 272 to 155 m^2/g. The presence of the heteropolyacid structure in HPA/SiO_2 samples after impregnation and calcination was confirmed by comparing their XRD patterns with that of pure HPA. An incipient phase of $H_3PW_{12}O_{40} \cdot xH_2O$ was detected for loadings above 30 wt.%, as previously reported [13]. The XRD pattern of the Cs-HPA sample agreed with those reported in the literature [14].

The nature, density and strength of surface acid sites were determined from the IR spectra of adsorbed pyridine after admission at 298 K and sequential evacuation at increasing temperatures. Figure 1 shows the IR spectra obtained on samples of Table 1 after evacuation at 423 K. The SiO_2 support was not acid while bulk HPA showed

Table 1 Surface area, sample acidity and catalytic results for ionone synthesis

Catalyst	Surface area (m^2/g)	IR spectroscopy of adsorbed pyridine[c]		Catalytic results[d]					
		B (area/g)	L (area/g)	r^0_{IONONE} (μmol/hg)	X^e_{PS} (%)	η^e_{IONONE} (%)	Ionone isomer distribution[e] (%)		
							α	β	γ
HPA/SiO_2[a]	155	161	15	3,270	87.9	58.4	38.7	21.2	40.1
Amberlyst 35W	39	–	–	1,400	88.7	49.1	55.3	27.0	17.7
Cs-HPA[b]	143	103	10	1,380	38.3	25.1	33.8	28.9	37.3
HBEA	630	195	203	252	20.1	7.7	48.9	12.8	38.3
SiO_2–Al_2O_3	560	36	145	353	21.8	5.3	41.8	54.5	3.7
HPA	9	473	0	62	3.9	1.2	46.7	0.0	53.3

[a] HPA loading = 42.5 wt.%; [b] Cs^+ content = 11.0 wt; [c] Data obtained after pyridine admission at 298 K and evacuation at 423 K, B: Brønsted sites, L: Lewis sites; [d] Reaction conditions: T = 353 K, P = 250 kPa, n^0_{PS} = 0.009 mol, Toluene/PS = 71 (molar ratio), W_{CAT} = 1.0 g; [e] At t = 6 h

exclusively the bands typical of pyridinium ion formed on strong Brønsted (B) acid sites (1,636 and 1,537 cm^{-1}) [15]. The other spectra in Fig. 1 exhibited additional bands at 1,622 and 1,455 cm^{-1} corresponding to pyridine coordinated on Lewis (L) acid sites [15]. Since the pyridine molar absorption coefficients on the solids of Table 1 were not available, the relative contributions of Lewis and Brønsted acid sites were obtained by deconvolution and integration of pyridine absorption bands appearing in Fig. 1 at around 1,455 and 1,540 cm^{-1}, respectively. Results are presented in Table 1. In addition, the B/L ratio upon pyridine evacuation at increasing temperatures is presented in Fig. 2. Zeolite HBEA contained a high density of surface acid sites and the B/L ratio was close to one after evacuation at 423 K. In contrast, SiO_2–Al_2O_3 presented essentially Lewis acidity showing a B/L ratio of 0.25 at that same evacuation temperature. The B/L ratio on zeolite HBEA decreased markedly with the evacuation temperature thereby indicating that this zeolite does not contain strong Brønsted acid sites. On SiO_2–Al_2O_3, the B/L ratio remained almost constant after pyridine evacuation at increasing temperature because this sample contains Brønsted and Lewis acid sites of similar strength.

Pure HPA exhibited the highest density of surface Brønsted sites (Table 1). Cs-HPA and HPA/SiO_2 samples displayed also essentially Brønsted acidity, showing B/L ratios of 10.3 and 15.0, respectively. The presence of pyridine adsorbed on Lewis acid sites of the HPA/SiO_2 sample (Fig. 1) suggests that upon impregnation of HPA on SiO_2, the heteropolyacid partially transforms giving rise to lacunary or unsaturated species of Lewis acid character formed by interaction with the silica support [13]. The B/L ratio on HPA/SiO_2 increased with the pyridine evacuation temperature, Fig. 2, thereby revealing the stronger acidity of the Brønsted sites in comparison to the Lewis acid sites.

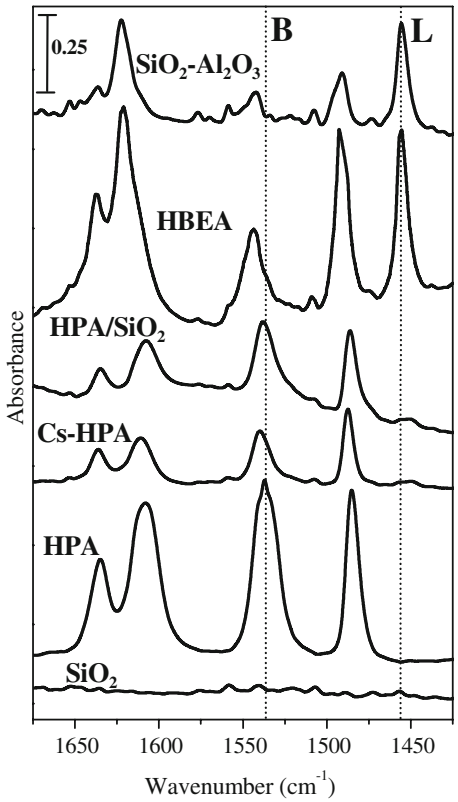

Fig. 1 FTIR spectra after pyridine adsorption at 298 K and evacuation at 423 K on different catalysts. B: Brønsted; L: Lewis. Signals normalized to 20-mg wafers

The catalytic performance of the different solid acids during PS cyclization to ionones was evaluated under identical reaction conditions; results are given in Table 1. Bulk HPA was almost inactive in spite of containing the highest density of Brønsted acid sites. This result indicates that the compact three-dimensional structure of HPA impedes the access of the PS molecules to the active

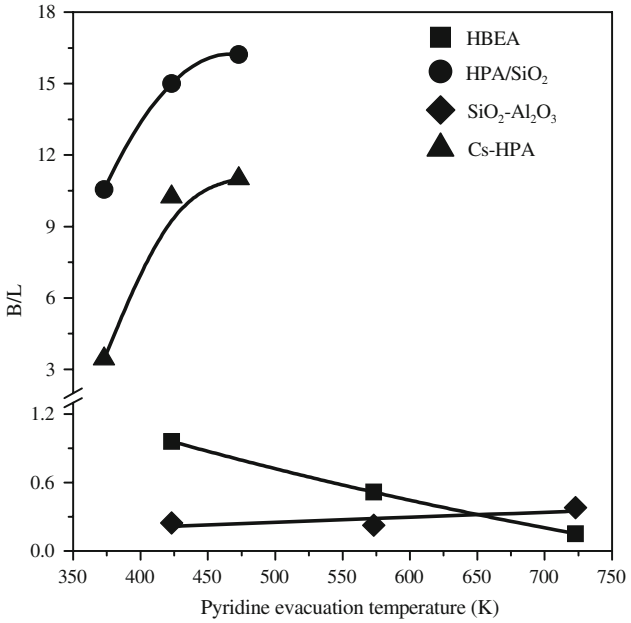

Fig. 2 Brønsted/Lewis acid site ratio from FTIR of pyridine adsorbed at 298 K on different catalysts and evacuated at increasing temperatures

centers of the solid. Even though its lower number of acid sites compared to HPA, the Cs-HPA sample displayed a 20-fold increase of the r^0_{IONONE} probably because the high surface area generated by substitution of Cs^+ for H^+ comes along with a more open structure. Nevertheless, X_{PS} and η_{IONONE} were only 38.3 and 25.1%, respectively, on Cs-HPA at the end of the 6-h catalytic test. Zeolite HBEA was clearly less active than Cs-HPA for converting PS, and X_{PS} on HBEA reached ~20% after the 6-h reaction. Since the PS molecular size (~9 Å) closely matches the HBEA channel size, the poor catalytic activity of this sample probably reflects the diffusional and spatial constraints for PS cyclization rather than being a consequence of the acid properties. SiO_2–Al_2O_3 does not present diffusional limitations for the reaction but it was also a poorly active sample. Because SiO_2–Al_2O_3 contains essentially Lewis acidity, one must conclude that the PS cyclization is not promoted on surface Lewis acid sites under the reaction conditions used in this work.

Amberlyst 35W and HPA/SiO_2 were the most active catalysts, reaching both about 90% PS conversion after the 6-h run. This result clearly suggests that the PS conversion is promoted on strong Brønsted acid sites. Although the acid properties of Amberlyst 35W could not be characterized by pyridine adsorption due to the low thermostability of this polymer, it must be noted that according to the manufacturer it contains ≥5,200 μmol H^+/g, which is clearly a higher proton density in comparison to a value of 440 μmol H^+/g corresponding to the HPA/SiO_2 sample. However, the highest ionone yield (η_{IONONE} = 58.4%) was obtained on HPA/SiO_2, probably reflecting that this sample not only contains a high density of strong Brønsted acid sites but also it is a high surface area material with no steric hindrance for PS cyclization.

Regarding the ionone isomer distribution on the most active samples, Table 1 shows that Cs-HPA and HPA/SiO_2 formed similar amounts of α and γ-ionones, between 34 and 40%, and to a lesser degree β-ionone. In contrast, on Amberlyst 35W α-ionone was clearly the major isomer, reaching 55.3% at the end of the catalytic test.

In summary, the results in Table 1 show that HPA/SiO_2 is a promising catalyst for the PS cyclization reaction that produced the highest ionone yield. We selected then this catalyst to perform additional studies with the aim of improving further the ionone formation rate from PS.

3.2 Ionone Synthesis on HPA/SiO_2 Catalysts. Effect of Reaction Temperature and Time, Solvent and HPA Loading

The effect of different experimental variables such as reaction temperature, solvent, heteropolyacid loading and reaction time was investigated on HPA/SiO_2 catalysts for the PS cyclization to ionones. Results are presented in Table 2.

A fivefold enhancement of the initial ionone formation rate was observed when the reaction temperature was increased from 353 to 373 K on the 42.5 wt.% HPA/SiO_2 catalyst (entries 1 and 2 of Table 2). The temperature increase also changed the ionone isomer distribution. In fact, at similar PS conversions (≈78%, entries 1a and 2a), the ionone yield was almost the same at both temperatures but the contribution of the α isomer was remarkably enhanced at expenses of the γ isomer at 373 K. The PS conversion reached 100% after 1.7 h reaction at 373 K, but the ionone yield slightly decreased afterward as a result of ionone decomposition with formation of light unknown compounds (entries 2b and 2c).

The PS cyclization was also studied on 42.5 wt.% HPA/SiO_2 catalyst at 373 K using two different non polar solvents (toluene and cyclohexane), taken into account that it is well known that HPA is soluble in polar solvents. Table 2 shows that at 373 K r^0_{IONONE} was about two times higher in toluene (entries 2 and 3 of Table 2). As a consequence, the reaction length required to reach 100% PS conversion was lower in toluene (1.7 h) than in cyclohexane (5 h) (entries 2b and 3a). In contrast, at X_{PS} = 100% η_{IONONE} was slightly higher in cyclohexane. Also, the drop of the η_{IONONE} at high reaction times due to the formation of light unknowns was less noticeable in cyclohexane.

The effect of HPA content on HPA/SiO_2 activity and selectivity was studied by varying the HPA loading

Table 2 Effect of experimental variables on the catalytic performance of 42.5 wt.% HPA/SiO_2 catalyst

Entry #	Reaction temperature (K)	Solvent	Catalytic results[a]						
			r^0_{IONONE} (μmol/hg)	Time (h)	X_{PS} (%)	η_{IONONE} (%)	Ionone isomer distribution (%)		
							α	β	γ
1	353	Toluene	3,270						
1a				4.2	78.3	52.8	37.2	20.2	42.6
2	373	Toluene	17,140						
2a				0.4	78.4	54.9	51.1	18.8	30.1
2b				1.7	99.7	69.3	59.0	18.2	22.8
2c				6.0	100.0	65.2	65.6	17.7	16.7
3	373	Cyclohexane	9,640						
3a				5.0	99.9	73.0	51.8	25.1	23.1

[a] Reaction conditions: $n^0_{PS} = 0.009$ mol, Solvent/PS = 71 (molar ratio), $W_{CAT} = 1.0$ g

between 18.8 and 58.5 wt.%. The resulting surface areas decreased with the HPA loading in the range of 208 to 155 m^2/g probably due to formation of an incipient three-dimensional HPA structure that partially blocks the silica pores. From the FTIR spectra of adsorbed pyridine on HPA/SiO_2 samples (not shown here), the intensity of the band corresponding to pyridine adsorbed on Brønsted acid sites was found to continuously increase with the HPA loading (Fig. 3a). Then, HPA was highly dispersed on the silica support even at high HPA loadings, what is reflected in an almost complete accessibility of the surface protons for pyridine adsorption.

The relative contribution of the Brønsted acid sites, which is presented as B/(B + L) in Fig. 3a, also increased with the HPA content. Therefore, increasing the HPA loading in HPA/SiO_2 samples enhances both the density of Brønsted acid sites and the sample average acid strength.

The catalytic performance of the HPA/SiO_2 catalysts with different HPA loadings is compared in Fig. 3b at the end of the 6-h run at 353 K. As a result of the enhanced acid site density and strength, the ionone yield monotonically increased with the HPA content, reaching 68% for the 58.5 wt.% HPA/SiO_2 catalyst. An additional experiment was carried out by testing the 58.5 wt.% HPA/SiO_2 sample at 383 K. It is observed in Fig. 3b that this sample yielded 79% ionones at 383 K after just 1.5 h of reaction time. This ionone yield is comparable to those reported for the homogeneously-catalyzed PS cyclization [3–7] and opens therefore a good perspective for the use of solid catalysts to synthesize ionones.

Finally, it must be remarked that the ionone isomer distribution can be controlled not only by the reaction temperature but also by the PS conversion and the reaction time, since interconversion of the isomers was in some cases observed during reaction. Although the three isomers were primary products formed directly from PS at low

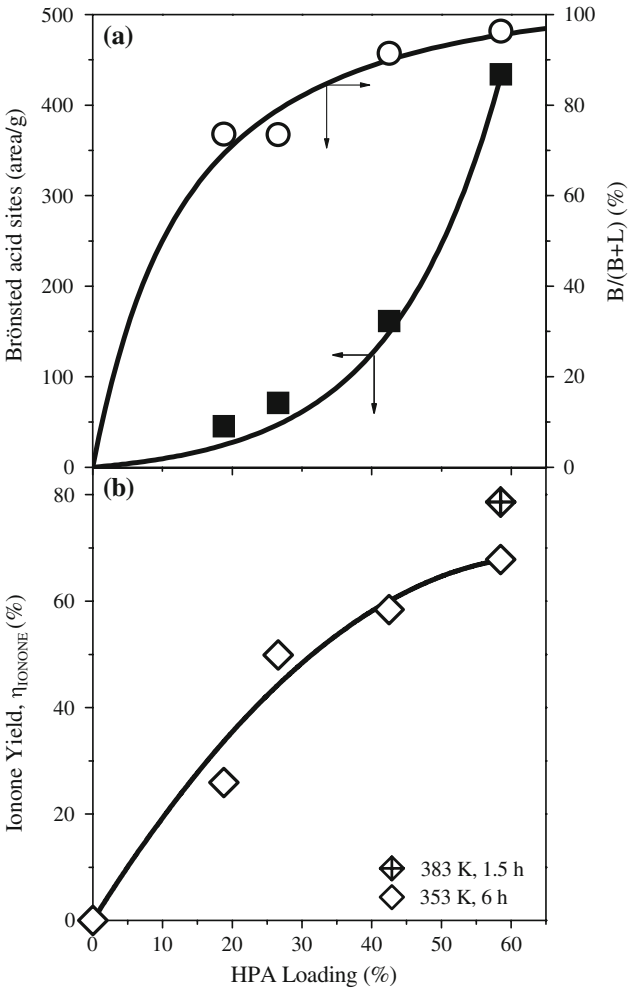

Fig. 3 Effect of the HPA loading on HPA/SiO_2 acidity and activity. (**a**) Density and relative contribution of Brønsted acid sites [from FTIR of pyridine adsorbed at 298 K and evacuated at 423 K]; (**b**) Ionone yield [$n^0_{PS} = 0.009$ mol, Toluene/PS = 71 (molar ratio), $W_{CAT} = 1.0$ g]

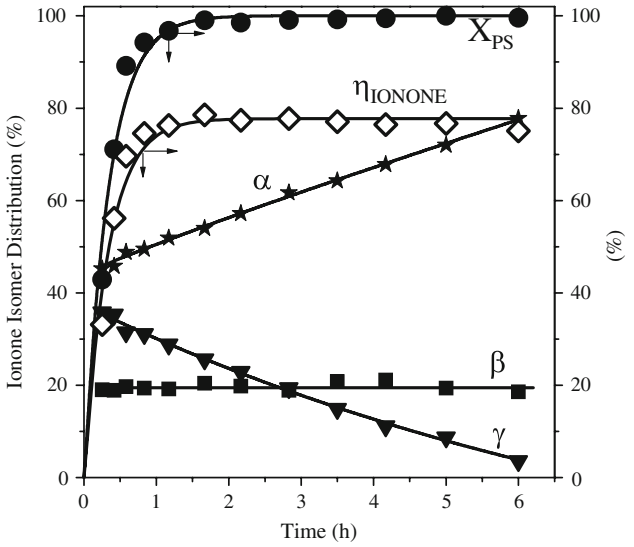

Fig. 4 PS conversion (X_{PS}), Ionone yield (η_{IONONE}) and Ionone isomer distribution as a function of time. [58.5 wt.% HPA/SiO_2, $T = 383$ K, $n^0_{PS} = 0.009$ mol, Toluene/PS = 71 (molar ratio), $W_{CAT} = 1.0$ g]

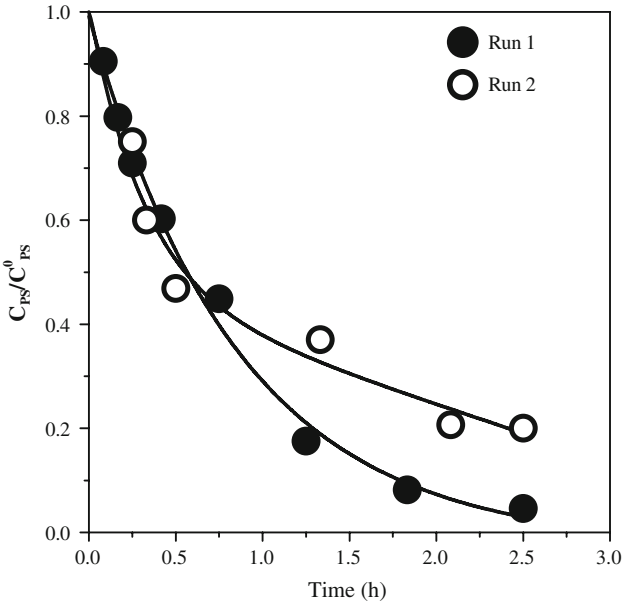

Fig. 5 Relative PS concentration in consecutive catalytic runs to evaluate in-situ catalyst deactivation [42.5 wt.% HPA/SiO_2, $T = 353$ K, $n^0_{PS} = 0.009$ mol, Toluene/PS = 71 (molar ratio), $W_{CAT} = 2.0$ g]

temperatures (343–353 K), at 383 K isomer transformation occurred. Figure 4 shows the isomer distribution as a function of time on 58.5 wt.% HPA/SiO_2 at 383 K. It is observed that a complete PS conversion and an ionone yield of 79% were obtained at 1.5 h, but at longer reaction times the contribution of the α isomer continuously augmented at expenses of the γ isomer, from 54% at 1.5 h to 78% at the end of the 6-h run. Transformation of the γ isomer is some way expected considering the instability and reactivity of this isomer due to the exocyclic C=C bond (Scheme 1). In contrast, the β isomer stabilized by the presence of the conjugated system, is produced directly from PS with almost constant selectivity.

3.3 Deactivation of HPA/SiO_2 catalysts

The in-situ catalyst deactivation was studied on the 42.5 wt.% HPA/SiO_2 sample by performing two consecutive catalytic tests without stopping the run. The procedure was as follows: after 2.5 h of reaction at 353 K and 250 kPa, an additional amount of PS was introduced so that the total moles of PS in the reactor at that point were equivalent to the initial moles of PS loaded to the reactor, n^0_{PS}, and a second consecutive run was then performed. Results are shown in Fig. 5. The PS concentration (C_{PS}) decay rate was slower in the second run in comparison with the first one thereby reflecting the partial sample deactivation. In fact, in the first run the PS conversion after 2.5 h was 95% but it dropped to 80% at the end of the second one; the ionone selectivity on the other hand, remained almost unchanged.

Deactivation of the 42.5 wt.% HPA/SiO_2 sample during the PS cyclization reaction cannot be attributed to heteropolyacid leaching to the liquid phase. In effect, we confirmed the lack of leaching during reaction in toluene or cyclohexane by monitoring in the liquid phase the UV band of the Keggin anion at 260 nm [16]. Therefore, the catalyst deactivation is more likely caused by the strong adsorption of PS and/or reaction products or by deposition of carbonaceous fragments formed by cracking of them.

4 Conclusions

The liquid-phase synthesis of ionones by pseudoionone cyclization can be efficiently achieved on solid acids containing a high density of surface Brønsted acid sites such as Amberlyst 35W and silica-supported heteropolyacids. HPA/SiO_2 catalysts are specially active and selective for this reaction giving ionone yields comparable to those obtained via the homogeneous synthesis. The superior performance of HPA/SiO_2 catalysts is due not only to their strong Brønsted acidity but also to the fact that they are high surface area materials with no steric hindrance for PS cyclization.

Ionone synthesis is more favorably carried out at high reaction temperatures, on high-loading silica-supported heteropolyacids and using toluene as a solvent. Ionone isomer distribution can be controlled by changing the

reaction conditions. In particular, the α isomer selectivity is enhanced at high reaction temperatures and reaction times.

Acknowledgments Authors thank the Agencia Nacional de Promoción Científica y Tecnológica (ANPCyT), Argentina (Grant PICT 14-11093/02), CONICET, Argentina (Grant PIP 5168/05) and the Universidad Nacional del Litoral, Santa Fe, Argentina (Grant CAI+D 007-040/05) for the financial support of this work. They also thank Prof. P. E. Mancini for useful discussions and H. Cabral and B. Marcos for technical assistance.

References

1. Ullmann's Encyclopedia of Industrial Chemistry, 6th edn. 2002 (electronic)
2. Brenna E, Fuganti C, Serra S, Kraft P (2002) Eur J Org Chem 967
3. Hibbert H, Cannon LT (1924) J Am Chem Soc 46:119
4. Royals EE (1946) Ind Eng Chem 38:546
5. Hertel O, Kiefer H, Arnold L (1986) US Patent 4,565,894, to BASF Aktiengesellschaft
6. Rheude U, Horcher U, Weller D, Stroezel M (2001) US Patent 6,288,282, to BASF Aktiengesellschaft
7. Steiner K, Ertel H, Tiltscher H (1995) US Patent 5,453,546, to Hoffmann-La Roche Inc
8. Ohloff G, Schade G (1963) Angew Chem Int Ed 2:149
9. Lin Z, Ni H, Du H, Zhao C (2007) Catal Commun 8:31
10. Guo D, Ma Z-F, Jiang Q-Z, Xu H-H, Ma Z-F, Ye W-D (2006) Catal Lett 107:155
11. Freund H, Wright ML, Brookshier RK (1951) Anal Chem 23(5):781
12. Kozhevnikov I (1998) Chem Rev 98:171
13. Kozhevnikov IV, Kloetstra KR, Sinnema A, Zandbergen HW, van Bekkum H (1996) J Mol Catal A: Chem 114:287
14. Soled S, Miseo S, McVicker G, Gates WE, Gutierrez A, Paes J (1996) Chem Eng J 64:247
15. Bachiller-Baeza B, Anderson JA (2004) J Catal 228:225
16. Kimura M, Nakato T, Okuhara T (1997) Appl Catal A: Gen 165:227